Nanomaterial Synthesis and Integration for Sensor and Energy Applications

IEEE CPMT/SCV
8 May 2013

Heather Chiamori
Department of Aeronautics & Astronautics
Stanford University

Berkeley

XLab Extreme Environment Microsystems Laboratory

BSAC

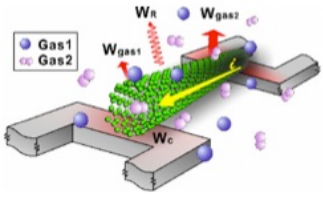

(I) Self-assembled, integrated electrothermal carbon nanotube gas sensor

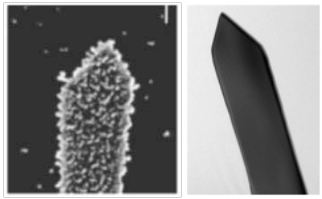

(II) Highly reactive facets of titanium dioxide nanoswords for energy and environmental applications

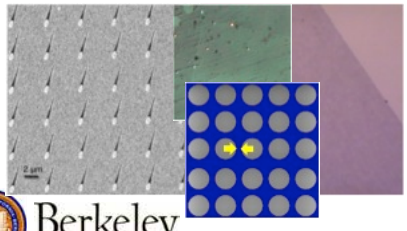

(III) Silver nanowires and graphene for biological and optical sensing

Berkeley

2

BSAC

Local synthesis addresses placement and integration of nanostructures

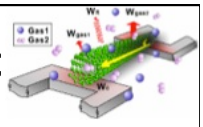

Selective locations for nanostructure growth

Integration of nanostructures with the macroscale

Microelectronics compatible

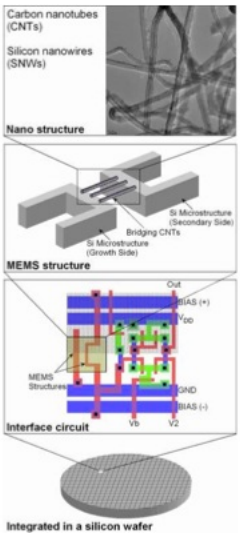

Berkeley

3

BSAC

Electrothermal CNT sensors based on pressure-dependent response

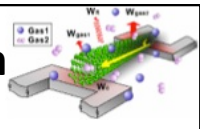

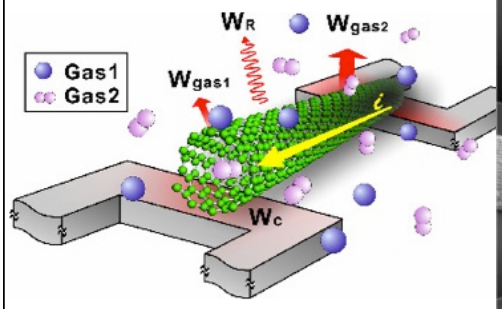

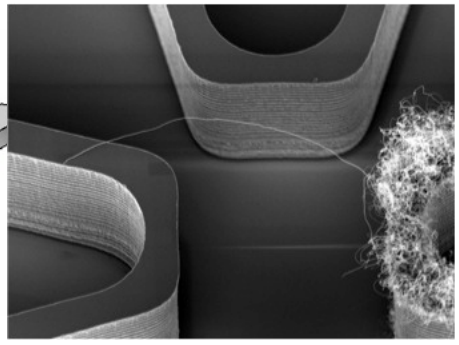

Energy conducted through the gas

$$W_G = \frac{1}{4}\frac{(\gamma+1)}{(\gamma-1)}\alpha\sqrt{\frac{2R}{\pi MT_{wall}}}\left(T_{CNT}-T_{wall}\right)p$$

T. Kawano, H. Chiamori, M. Suter, Q. Zhou, B. D. Sosnowchik, and L. Lin, Nanoletters, (7) 2007, 3686

Berkeley

4

BSAC

Low power CNT pressure sensor can operate on µW power

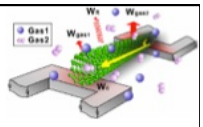

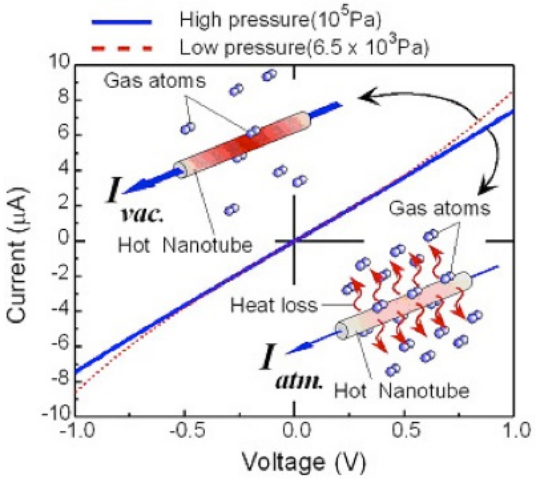

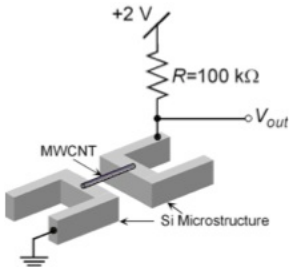

Berkeley

5

BSAC

CNT synthesis with local control over growth temperature

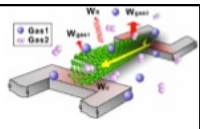

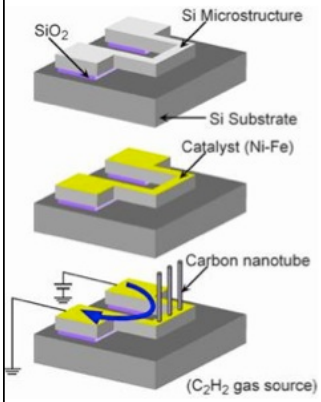

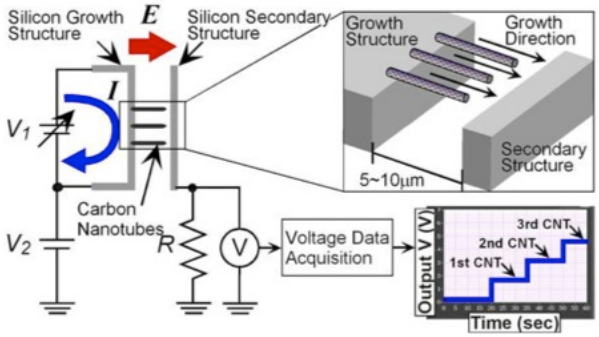

Berkeley

T. Kawano, C. Y. Cho, and L. Lin, 20th IEEE MEMS 2007, 831- 834.

6

BSAC

CNT chamber and experimental setup

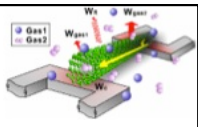

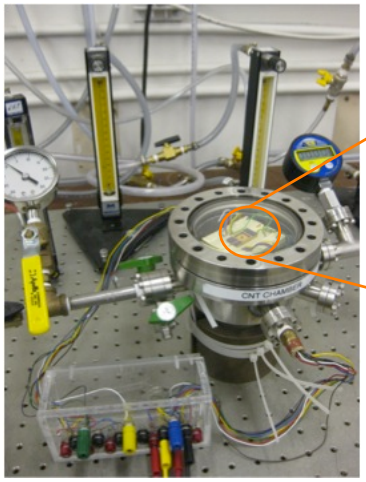

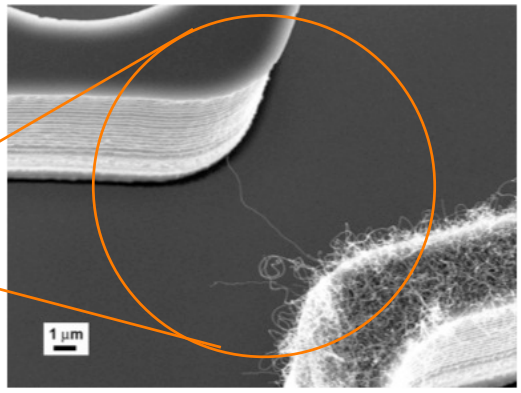

Silicon microbridge gap distances of 5 to 20 µm.

Berkeley

7

BSAC

CNT sensor demonstrates repeatable, rapid response to pressure change

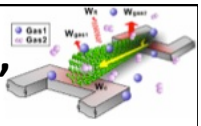

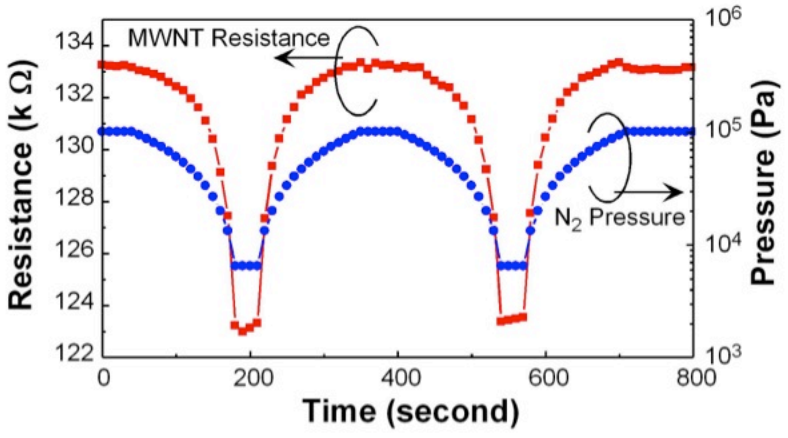

Berkeley

8

BSAC

CNT sensor baseline values can be determined from energy dissipation

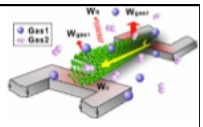

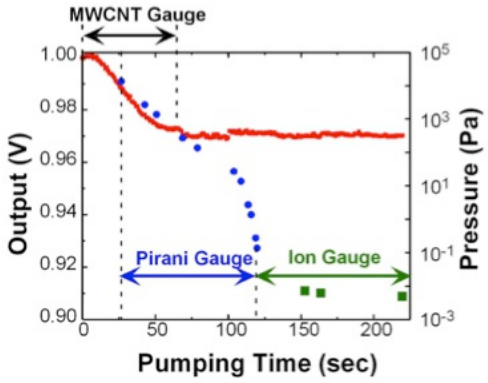

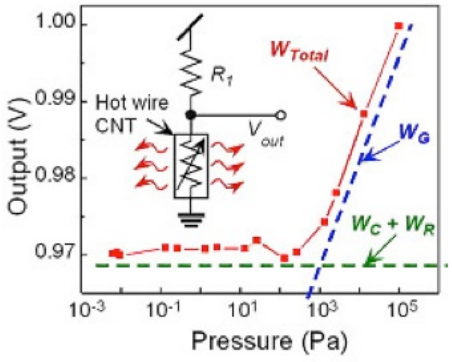

Berkeley

9

BSAC

Contact interface influences CNT power dissipation

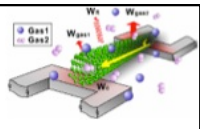

Energy dissipation can potentially determine the MWCNT thermal conductivity value

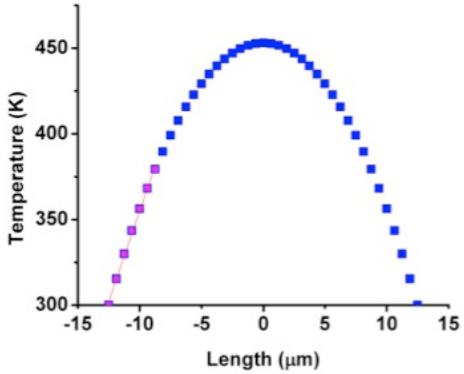

W_R	~ 20 nW
W_{TOTAL} Baseline	7.5 mW
k_{CNT} Vacuum T_{avg}=373K	300 W/mK

$$\frac{1}{2}W_C = k_{CNT} A \frac{dT_{CNT}}{dl}\Big|_{l=0}$$

Berkeley

10

BSAC

Potential of sensing different gas species

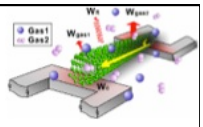

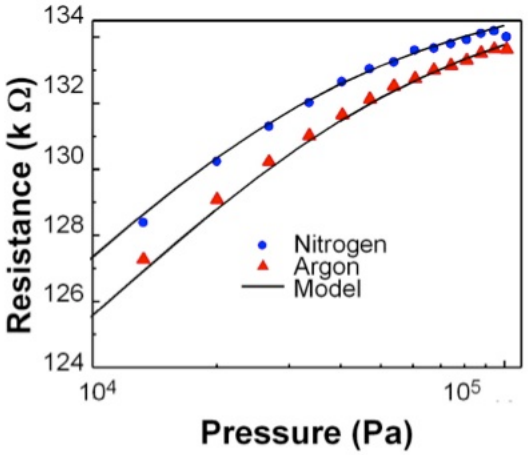

Berkeley

Improving the nano- to micro-contact resistance

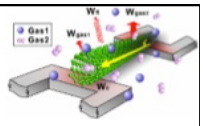

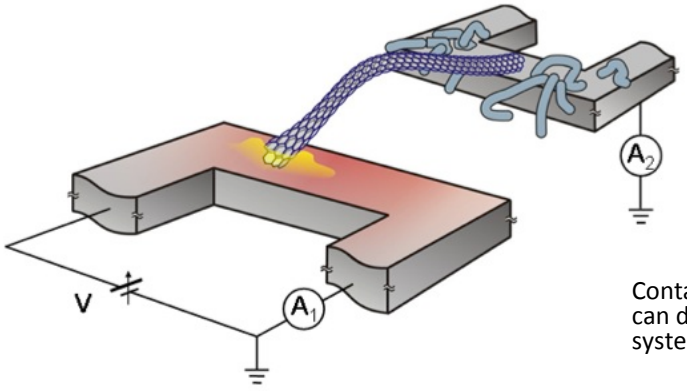

Contact resistance can dominate overall system resistance

$$R_{Total} = R_{growth} + R_{contact1} + R_{CNT} + R_{contact2} + R_{secondary}$$

Higher power annealing can reduce contact resistance

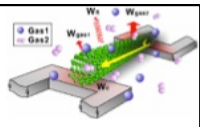

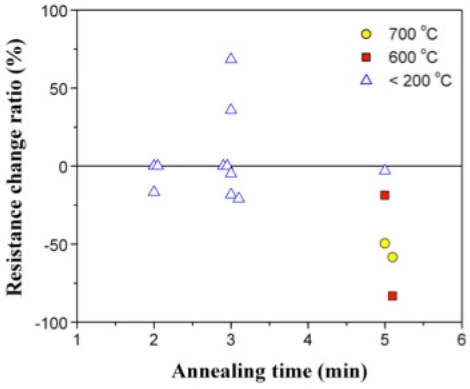

$$\text{Resistance Change Ratio } (\%) = \frac{R_{final} - R_{initial}}{R_{initial}} x100$$

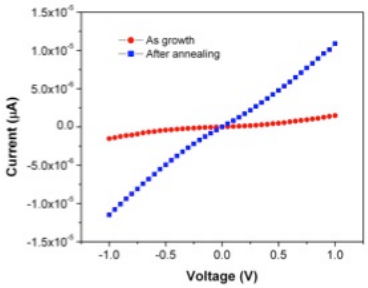

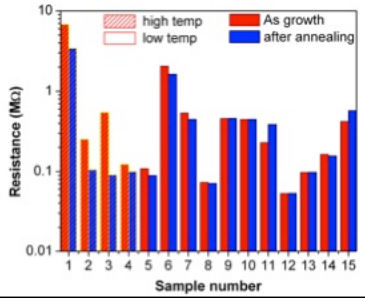

H Chiamori, X. Wu, X Guo, B. Ta, and L. Lin, 5th IEEE NEMS 2010.

13

Titanium dioxide is used for multiple energy and environmental applications

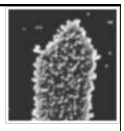

- Photocatalysis: UV-generated free-radicals enable "depollution"
- Photovoltaics: Dye-sensitized solar cells
- Hydrogen Generation: Water Splitting
- Sensor Apps: O_2, H_2, CO, and humidity sensors
- Lab-on-a-chip: cleaving peptides

Titanium dioxide window coatings for UV-activated self-cleaning windows

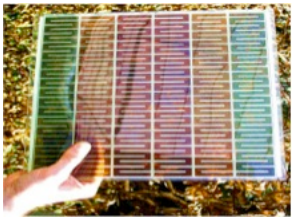

Dye-coated titanium dioxide solar panels

Berkeley

Image credits: anlin.com/infinit-e-plus.aspx; solarisnano.com

14

Induction heating synthesis method is rapid, clean, and occurs within minutes

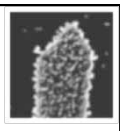

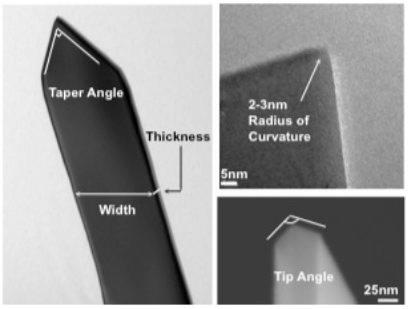

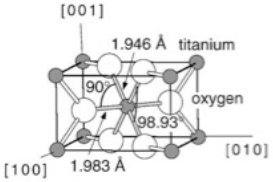

Rutile, Tetragonal
a=b=4.587 Å; c= 2.953 Å

TiO_2

- N-type semiconductor
- Three phases
  - Anatase
  - Rutile
  - Brookite
- Large band gap
  - Rutile 3.0 eV
  - Anatase 3.2 eV

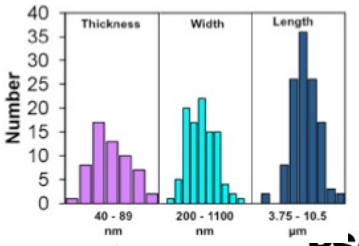

Berkeley

U. Diebold, Surf. Sci. Rep., (48) 53, 2003; B. D. Sosnowchik, J.-Y. Ha, L. Luo, and L. Lin, 21st *IEEE MEMS, 2008.*

15

BSAC

Certain crystalline TiO_2 facets exhibit higher photocatalytic activity

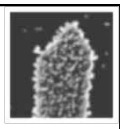

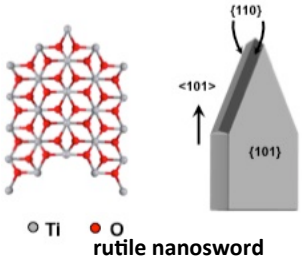

rutile nanosword

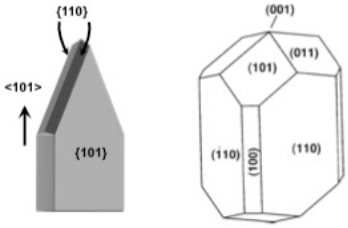

rutile

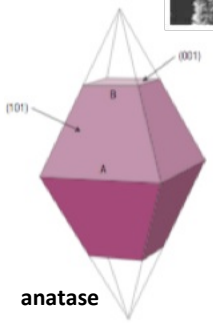

anatase

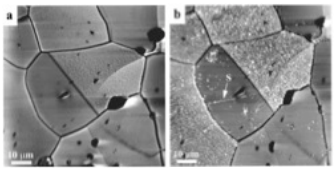

before (a) and after (b) the photochemical deposition of silver onto TiO_2.

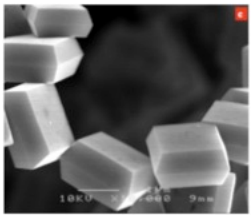

Engineered faces of anatase TiO_2.

Berkeley

Lowekamp, et. al, *J. Phys. Chem. B* **102**, 7323 (1998); M. Ramamoorthy, D. Vanderbilt, R. D. King-Smith, *Phys. Rev. B* ***49, 16721 (1994)***; H. G. Yang *et al., Nature* ***453****, 638 (2008)****;*** A. Selloni, *Nature Materials* **7**, 613 (2008).

16

BSAC

Facet-dependent photocatalysis experimental setup

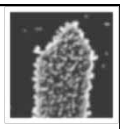

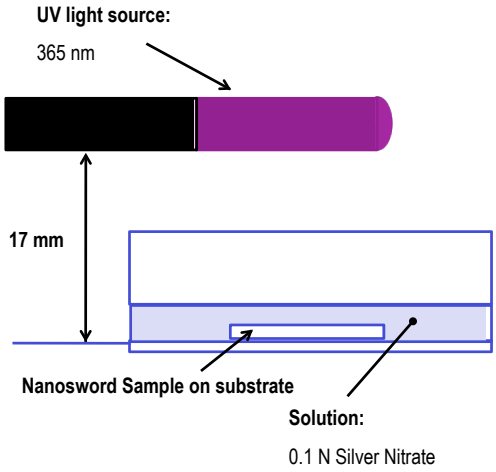

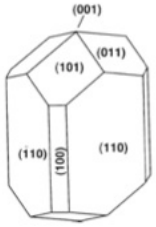

Control substrates:

TiO_2 (110)

TiO_2 (101)

Berkeley

17

BSAC

Silver reduction: 17 minutes

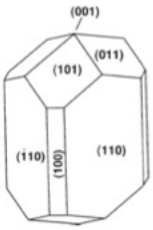

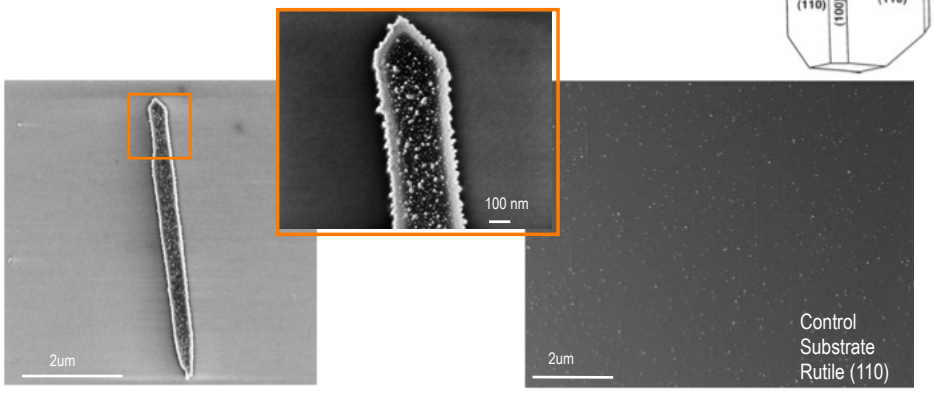

nanosword **control**

Berkeley

18

BSAC

Silver reduction: 1 hour

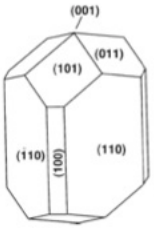

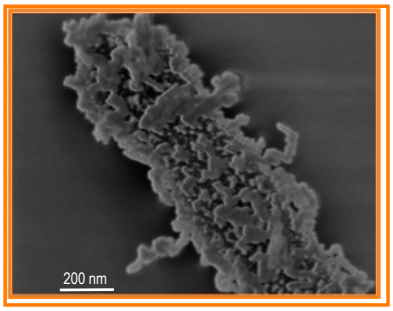

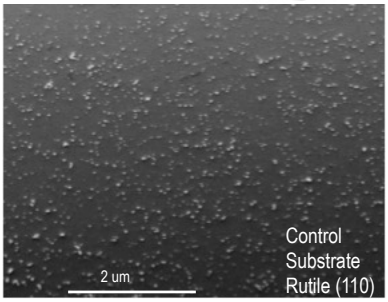

nanosword **control**

Berkeley

19 BSAC

Enhanced photocatalytic activity of TiO_2 nanoswords

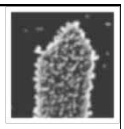

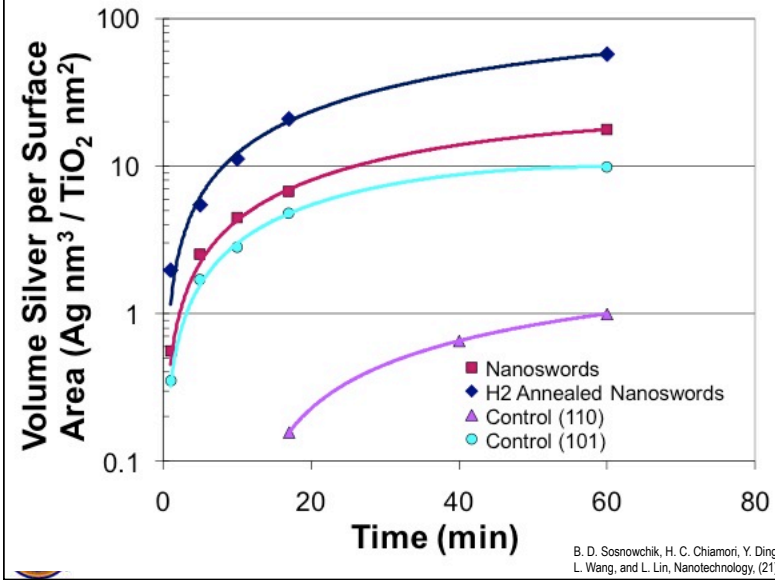

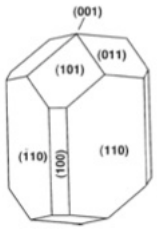

B. D. Sosnowchik, H. C. Chiamori, Y. Ding, J.-Y. Ha, Z. L. Wang, and L. Lin, Nanotechnology, (21), 2010

20 BSAC

Self-sourced, rapid synthesis of titania nanostructures and thin films

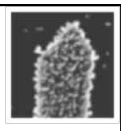

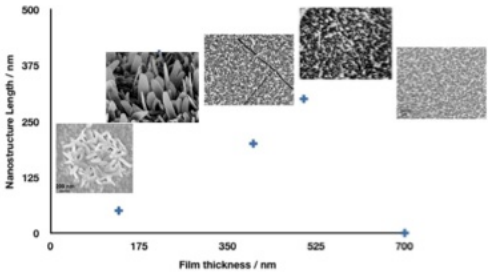

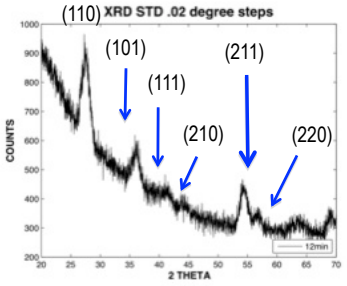

TiO_2 nanostructure length based on initial titanium thin film thickness. Substrates include quartz, metal, and silicon. Synthesis times range from 8-12 minutes.

XRD measurements indicate rutile titania material.

Berkeley

21

BSAC

Large area synthesis of silver nanowires using oblique angle deposition

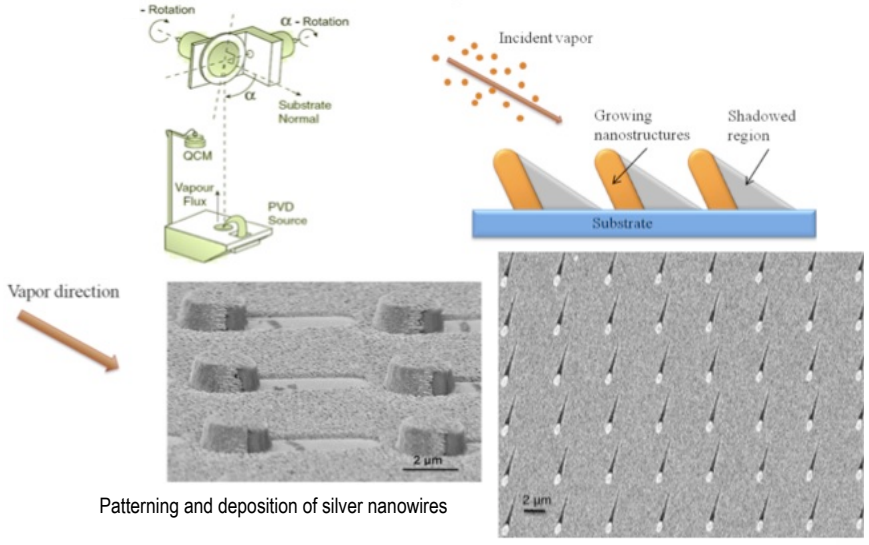

Patterning and deposition of silver nanowires

W Zheng, HC Chiamori,, L Lin and FF Chen, Plasmonic Nanostructures in Biosensing. In *Bionanotechnology II: Global Prospects* 2011; JJ Steele and MJ Brett, *J Mater Sci-Mater El* **2007,** *18* (4), 367-379.

22

BSAC

Next generation sensors for electrical and optical applications

- Advantages of nanostructures
  - Large surface-to-volume ratio
  - Increased sensitivity
  - Lower power consumption
- Graphene
  - Electrical devices
    - Ballistic transport at ambie
    - Extremely high mobilities
      - 200000 $cm^2V^{-1}s^{-1}$
      - >15,000 $cm^2V^{-1}s^{-1}$ at ambient
  - Tunable IR lasers and detectors
    - Bilayer graphene
  - Building up metamaterials using graphene
    - Biosensing (SERS, LSPR), optical sensing

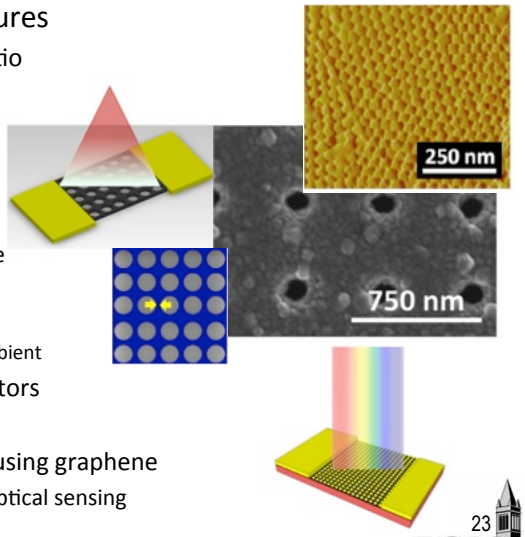

Berkeley

Yang, E., et al, JVST B (28) C6M93 2010; Yang, C, et al., JVST B (30) 02[illegible]

23 BSAC

Graphene is a nanomaterial with outstanding properties

- Semimetal
  - Dirac fermions, zero effective mass
- Charge carriers ballistic transport
  - Up to a micron at room temperature
- Mobilities as high as 200,000 $cm^2V^{-1}s^{-1}$
  - High frequency electronic devices
- Absorption 2.3% visible light
  - Transparent conductor, low resistance
- Inducing bandgap
  - Nanoribbons: confinement gap scales with width

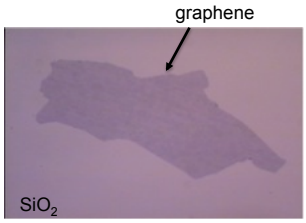

CVD graphene
*Copper foil (copper thin films)
*<u>**Large areas**</u>, <u>**high quality possible**</u>
*Mobilities up to 7350 $cm^2V^{-1}s^{-1}$ at low temp

24 BSAC

Nanoimprinting graphene provides multiple sensor configurations

Etching

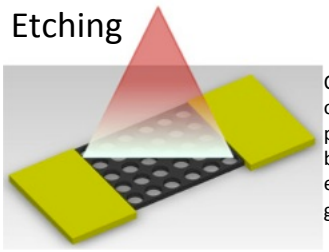

Optical and optoelectronic properties of bandgap engineered graphene

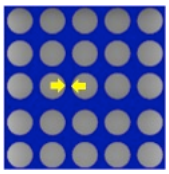

The bandgap of graphene nanoribbons scales with the width

Building up metamaterials

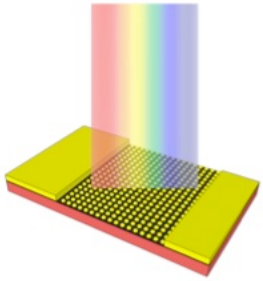

Optical bio- and chemical sensing using localized surface plasmon resonance (LSPR) and surface enhanced Raman spectroscopy (SERS)

Berkeley

25

BSAC

Summary and future work

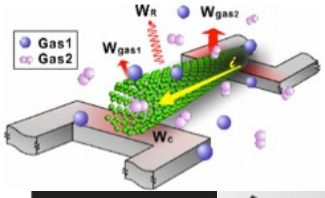

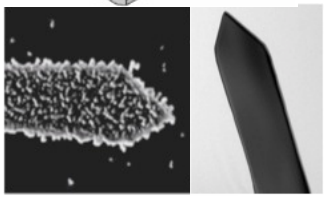

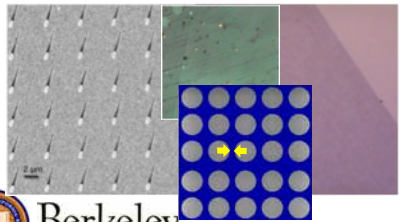

(I) Self-assembled, integrated electrothermal carbon nanotube gas sensor

- Demonstration of CNT thermal resistive pressure sensor
- Potential gas species differentiation possible with CNT device
- Localized synthesis and direct integration of CNTs for microelectronics compatible devices
- Annealing for improved electrical contact resistance

(II) Highly reactive facets of TiO_2 nanoswords for energy and environmental applications

- Demonstration of higher photocatalytic reactivity compared to control substrates
- Solar absorption increase based on thermal annealing
- Furnace-based approach for bulk TiO2 nanostructure growth

(III) Silver nanowires and graphene for biological and optical sensing

- Silver nanowire growth based on oblique angle deposition with morphology control
- Test platform for SERS and biosensing
- Graphene bandgap engineering for additional device functionality
- Electrical and optoelectronic applications

Berkeley

26

BSAC

Acknowledgments

- UC Berkeley: Prof. Liwei Lin, Dr. Brian Sosnowchik, Dr. Jong-Yoon Ha, Dr. Taku Hirasawa, Jonas Lin, Dr. Ming-Tsang Lee, Dr. Sara Beaini, Dr. Adrienne Higa, Dr. Vi Rapp, Prof. Oscar Dubon, Prof. John Clarke, Prof. Al Pisano
- Prof. Takeshi Kawano, Marcel Suter, Prof. Xiaoming Wu, Prof. Xishan Guo, Bao Quoc Ta, Adam Resnick, Jim Gao, Chung Yeung Cho, Dr. Yingqi Jiang, Dr. Qin Zhou, Dr. Ryan Yang, Dr. Lei Luo, Dr. Choongho Yu, Dr. Woochul Kim, Dr. Dane Christensen, Dr. Ongi Englander, Dr. Jiyoung Chang, Dr. Armon Mahajerin, Kevin Limkrailassiri, Roseanne Warren, Dr. Ryan Sochol, Kosuke Iwai, Dr. Erika Parra, Alina Kozinda, Matt Chan, The Lin Lab
- LBNL: Prof. Samuel Mao, Dr. Coleman Kronawitter, Dr. Frank Chen, Dr. Wenwei Zheng, Dr. Tim Suen, Dr. Shaohua Shen; Georgia Tech: Dr. Yong Ding, Prof. Zhong Lin Wang; Siemens Corp., DARPA N/MEMS S&T
- Work at the Molecular Foundry was supported by the Office of Science, Office of Basic Energy Sciences, of the U.S. Department of Energy under Contract No. DE-AC02-05CH11231.
- UC Berkeley Marvell Nanofabrication Laboratory and staff; BSAC
- Sandia National Laboratories: Dr. Jack Skinner, Dr. Elaine Yang, Dr. Peter Yang, Chip Steinhaus, David Heredia, Dr. Francois Leonard, Dr. Aaron Katzenmeyer, Dr. Lexi Ford, Dr. Alexander Kane, Douglas Gehmlich, NSF/SNL NINE summer program 2011
- NSF Graduate Research Fellowship
- Stanford University: Prof. Debbie G. Senesky

Berkeley

XLab Extreme Environment Microsystems Laboratory

BSAC

Thank you!